Modeling and Design of an Indirect Air Conditioning System Operating With Low GWP Zeotropic Mixtures

Marian Hamdar
Ecole des Mines de Paris

Assaad Zoughaib
Ecole des Mines de Paris

Denis F. F. Clodic
Ecole des Mines de Paris

MODELING AND DESIGN OF AN INDIRECT AIR CONDITIONING SYSTEM OPERATING WITH LOW GWP ZEOTROPIC MIXTURES

Marian HAMDAR[1]*, Assaad ZOUGHAIB[2], Denis CLODIC[3]

[1,2,3]Center of Energy and Processes, Ecole des Mines de Paris,
60, boulevard Saint Michel - 75272 Paris Cedex 06, France

[1]Phone: +33-1-40519405, Fax : +33-1-46342491
Email adress: marian.hamdar@ensmp.fr
[2]Phone: +33-1-40519466, Fax : +33-1-46342491
Email adress: assaad.zoughaib@ensmp.fr
[3]Phone: +33-1-40519249, Fax : +33-1-46342491
Email adress: denis.clodic@ensmp.fr

ABSTRACT

Indirect air conditioning can be considered as one of the technical options to reduce the refrigerant charge in order to minimize the emissions to the atmosphere. However, indirect systems are less efficient than direct ones due to the additional irreversibilities in the heat exchangers and the power consumption of the pumps. This problem can be overcome by the use of energy efficient heat exchangers with reduced approach temperature (1 K) and the choice of an efficient secondary fluid with evaluated thermo-physical properties. This paper deals with the modeling and design of an indirect air-conditioning system adapted to fluids with temperature glide. A particular attention is paid to the design of the primary and secondary heat exchangers by taking advantage of the mini-channels technology. The optimized heat exchanger presents high thermal efficiency, minimized pressure drop, and compactness over a conventional technology. The energy efficiency of the indirect system is calculated and comparison is carried out with a conventional direct system in order to predict the reduction of equivalent CO_2 emissions.

1. INTRODUCTION

The environmental issues related to global warming bring up a new concern over the use of HCFC and HFC refrigerants with high GWP. In the framework of refrigerant substitution, various fluids, for example HCs, HFCs and certain blends of HFCs, which are mostly flammable, are considered as possible candidates. The main concern over using these refrigerants remains however the flammability issue for safety reasons.

For mobile refrigeration and air conditioning, flammable alternatives require the use of single or double indirect loops to transport cold/heat via a safe secondary fluid or heat transfer fluid. The flammable or slightly flammable refrigerant is confined into a compact refrigeration loop. The refrigerant charge is reduced and possible leaks into the atmosphere are drastically reduced by the use of full hermetic compressor and a reduction of the number of fittings.

The study falls into the context of substitution of a direct expansion air conditioning system, used for a mobile application, by a double indirect one, operating with low GWP zeotropic refrigerant blends. The system is characterized by the introduction of mini-channels technology into the primary heat exchangers. A model has been developed to assist the design of the system components. This paper describes the main characteristics of the model, and particularly the mini-channel heat exchangers models. The results are presented in terms of system efficiency and compactness of the components.

2. SYSTEM DESCRIPTION

A double indirect air-conditioning system is composed of a primary refrigeration loop and two secondary loops from the evaporator and the condenser (Figure 1). Cold and hot heat transfer fluids (HTF) circulate in the evaporator/condenser loops and transfer heat to and from the refrigerant in the primary heat exchangers. Primary heat exchangers are Refrigerant-to-HTF plate heat exchangers. Secondary heat exchangers are Air-to-HTF parallel flow exchangers. They are referred to as cooler and heater. Cooled air is blown into the temperature control volume and the air blown through the radiator is rejected outdoor.

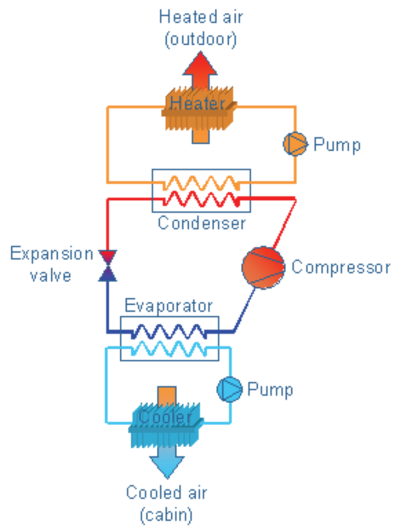

Figure 1: Indirect air-conditioning primary and secondary loops

The use of zeotropic refrigerant mixtures may result in improvement of the cycle coefficient of performance. The gain of performance can be illustrated by a comparison of the Carnot and Lorenz cycles. Theoretically, the cycle efficiency can be improved by reducing the temperature difference between refrigerant and heat transfer fluid, by achieving a temperature glide (TG) matching (Mulroy, 1994). The irreversibilities are reduced by maintaining a constant and small temperature difference along the heat transfer. For a specified cooling or heating duty, temperature glide matching with a specified mixture can only be obtained for a single mass flow rate of the heat transfer fluid. Besides its thermodynamic and transport properties, perfect glide matching is difficult to obtain for many zeotropic mixtures (Venkatarathnam, 1996). Unlike single-phase fluids, the refrigerant mixtures can present a non-linear temperature profile with enthalpy variation during phase change. The non-linearity property depends on the mixture composition and on the difference of normal boiling points between the constituents. An inappropriate mixture can result in non-linear temperature profile with a potential to show a pinch point between the two temperature profiles inside the evaporator or the condenser.
The last consideration is related to the evaporation and condensation heat transfer coefficients of zeotropic refrigerant mixtures. It is known that the heat transfer coefficient of mixtures is lower than that of pure components, if a linear mixing law is applied (Thome, 1996).

All of abovementioned issues show that the thermodynamic process obtained with zeotropes requires special care related to refrigerant selection and heat exchangers design. The required heat transfer areas with zoetropic blends are found to be larger to compensate the smaller temperature difference for TG matching and a possible lower heat transfer coefficient. Micro-channel tube heat exchangers represent an interesting technical option for compactness and heat transfer coefficient enhancement. This technology has been implemented in several industrial applications as automotive air conditioning, electronic cooling, waste heat recovery, etc.

In this study, the selected refrigerant is a binary mixture of R-152a and R-32, with respective mass percentage of 80% and 20%. The physical properties of refrigerants are presented in Table 1. The GWP of the mixture is 235.

Table 1: Pure components physical properties.

Refrigerant	Molecular mass (g/mol)	NBP (°C)	Tc (°C)	34 Std safety group	GWP (100 yr)
HFC-152a	66.05	-24	113.3	A2	124
HFC -32	52.02	-51.7	78.1	A2	675

3. SYSTEM MODELING

The indirect system model consists of primary refrigerant-to-HTF model, the secondary Air-to-HTF model, and a simple compressor model, based on the manufacturer data. External heat losses through the compressor, the refrigerant pipes, and the HTF pipes are not modeled. Calculation of the refrigerant thermodynamic and transport properties is performed with REFPROP 7.0 subroutines. Additionally, built-in polynomial functions, allow calculating the secondary fluid thermo-physical properties. Component models and physical assumptions are detailed in the following.

The heat exchanger zonal models involve mass and energy and momentum conservation equations. The energy equations are simplified by LMTD or ε-NUT approaches. The exchanger is discretized with a finite volume approach. The continuity of the refrigerant properties is verified in each unitary volume using special functions that check the state of the refrigerant through vapor quality. The set of equations is solved by iterations. Enthalpy and pressure are the variables calculated at the inlet and outlet of the elemental volume.

Figure 2 presents a layout of the heat exchanger model. Input data includes the heat exchanger type (primary or secondary), the flow configuration (cross-flow, co-current or counter-current), detailed heat exchanger geometry, and hot and cold flow inlet conditions. The model uses a library of heat transfer and pressure drop models and correlations. Adapted correlations are selected for each operating range and conditions. The model outputs are heat transfer rate, pressure losses, outlet state variables, temperature, pressure and heat transfer coefficients (HTC) variation profiles. The heat exchanger description is saved in an input file.

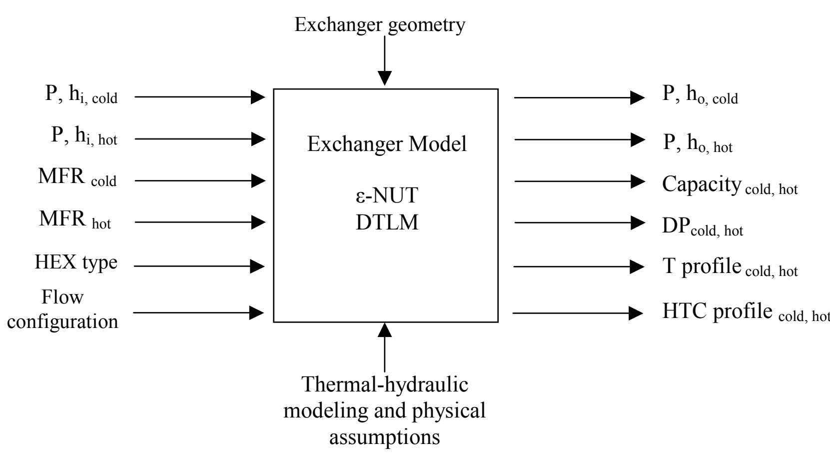

Figure 2 : Heat Exchanger model inputs and outputs.

3.1 Primary heat exchanger correlations

From the refrigerant side, the primary heat exchanger is designed with an assembly of multiport flat tubes, composed of several micro-channels, for the heat transfer coefficient enhancement. From the HTF side, the pressure drop is reduced by increasing the flow section area of HTF compared to the refrigerant in order to take into account the unbalanced mass flow rates between refrigerant and HTF in the evaporator and the condenser.

The prediction of boiling and condensation heat transfer coefficients in micro-channels is a highly studied issue. The experimental investigations have proven that the physical phenomena occurring in micro-scale channels are different from those occurring in macro-scale channels. The differences have been reported to be related to the effects of surface tension, gravity, and phase change mechanisms.

The heat transfer coefficients have been predicted through empirical correlations issued from a multitude of experimental data or validated physical models. The different prediction models have been reviewed, compared and discussed in a previous study.

Table 2: Two-phase heat transfer in mini-channels – Evaporation.

Authors	Channel size/ Fluid	Correlation	Parameter range
Thome et al. (Thome *et al.* 2004) (Dupont *et al.* 2004)	Comparison data: R-11, R-12, R-113, R-123, R-134a, R-141b and CO_2 D_h =0.77-3.1 mm	$h_{tot} = \frac{t_L}{\tau} h_L + \frac{t_{film}}{\tau} h_{film} + \frac{t_{dry}}{\tau} h_v$ Refer to Thome *et al.*	G = 50-564 kg/m²s Psat = 1.2-57.6 bar q''= 5-178 W/cm² x = 0.01-0.99

Recently, Bertsch et al. (Bertsch *et al.* 2008) measured boiling heat transfer coefficient of R-134a in a multi-channel evaporator. They presented the results for mass fluxes of 20, 40, 60, and 81 kg/m²s. The heat flux in their experiments varied from 0 to 20 W/cm². Their results are very important because they are representative of the refrigerant flow conditions in refrigeration and heat pumps systems. They observed maximum heat transfer coefficient at vapor quality of 20%. Their experimental results are consistent with Thome et al. (Thome *et al.* 2004) Being established for large geometry and parameter range database, and several refrigerants, the evaporation model of Thome et al. is selected for the prediction of the evaporation heat transfer coefficient (Table 2).

Table 3: Two-phase heat transfer in mini-channels – Condensation.

Authors	Channel size/ Fluid	Correlation	Parameter range
Wang et al. (Wang et al. 2002)	R-134a Rectangular multichannels D_h = 1.46 mm	$Nu_{all} = f_{annul} Nu_{annul} + (1 - f_{annul}) Nu_{strat}$ $Nu_{ann} = 0.0274 \Pr_l \mathrm{Re}_l^{0.6792} x^{0.2208} \left(\frac{1.376 + 8\chi_{tt}^{1.655}}{\chi_{tt}^2} \right)^{0.5}$ $Nu_{strat} = \alpha Nu_{film} + (1-\alpha) Nu_{conv}$ $Nu_{film} = 0.555 \left(\frac{\rho_l (\rho_l - \rho_v) g h_{fg} d_h^3}{k_l \mu_l (T_{sat} - T_w)} \right)^{1/4}$ $Nu_{conv} = 0.023 \mathrm{Re}_l^{0.8} \Pr_l^{0.4}$	Tsat = 45 – 66 °C x = 0.03 - 0.94 G=75-750 kg/m²s

Cavallini et al. (Cavallini *et al.* 2006) reviewed the condensation models and correlations for condensation in mini-channels. They compared experimental data from heat transfer coefficient measurement of R-134a and R410A (G = 400-1400 kg/m²s, x = 0.25-0.75) inside multi-port channels (Cavallini et al. 2005). They found that, for dimensional gas velocity lower than 2.5, the correlations of Wang et al. (Wang *et al.* 2002) and Koyoma et al. (Koyoma *et al.* 2002) can fairly well predict the heat transfer coefficient. For dimensional gas velocity greater than 2.5 (for shear dominated regimes), the Moser et al. model with the Zhang and Webb frictional pressure gradient suits better the heat transfer coefficient data. The tested fluids are pure refrigerants (R-134a, R-123, R-141b..) or near-azeotropic mixtures (R-410A). No data are found for condensation of zeotropic mixtures in mini-channels and the Wang et al. correlation is used in this study (Table 3).

3.2 Compressor and expansion valve modeling

The compression process is modeled using isentropic and volumetric efficiency. Adiabatic compression is assumed and thermal losses to the outside environment are neglected. The isentropic and volumetric efficiencies of the compressor are given as polynomial functions of the compression ratio (Equations 1 and 2). They are calculated based on the data provided by the manufacturer as follows:

$$\eta_v = -0.25\tau^2 - 1.33\tau + 101.53 \quad (1)$$

$$\eta_{is} = 0.021\tau^5 - 0.636\tau^4 + 7.603\tau^3 - 44.31\tau^2 + 120.249\tau - 50.6 \quad (2)$$

For a given discharge pressure, the compressor outlet enthalpy is given by Equation 4. The refrigerant mass flow rate is calculated using Equation 3, where D is the displacement rate.

$$\dot{m}_{ref} = \eta_v \frac{D}{v_{cpr,in}} \quad (3)$$

$$h_{cpr,out} = h_{cpr,in} + \frac{h_{cpr,out,is} - h_{cpr,in}}{\eta_{is}} \quad (4)$$

The expansion process of the refrigerant from the high pressure to the low pressure is assumed isenthalpic. Usually the volumetric flow rate through the expansion device is proportional to the differential pressure of the system. In this case, the mass flow rate through the expansion valve is assumed to be equal to that of the compressor.

3.2 Cycle simulation

The cycle simulation strategy consists of the following procedures.

First, the thermodynamic cycle is calculated with a cycle optimization tool that accounts for the TG matching between the refrigerant and the secondary fluid. The calculation tool is based on the "temperature pinch" method. In order to reduce irreversibility of the thermodynamic system, the temperature pinch is reduced to 2 K at the micro-channel (primary) heat exchangers and to 3 K at the secondary heat exchangers.
Inputs of the optimization tool are external air conditions (mass flow rate and temperatures), primary and secondary heat exchangers temperature pinch, and difference of temperatures for superheat and sub-cooling, compressor displacement rate. The cycle is optimized for temperature glide matching at the evaporator and the condenser. For a given required cooling capacity and a calculated refrigerant glide, temperature glide matching between the refrigerant and HTF only occurs only for one HTF mass flow rate. The compressor displacement rate is selected based on the cooling duty of the air-conditioning system. The subroutine allows defining the thermodynamic states of the refrigerant at the inlet and outlet of the heat exchangers and the compressor as well as the secondary fluid conditions.

Then, each of the primary and secondary heat exchangers is sized for the calculated operating conditions, in order to satisfy the cooling and heating duties. The sizing includes optimal design of the heat exchangers accounting for compactness of core volume, heat transfer enhancement, and pressure drop reduction. At this step, 4 input files describing geometry, inlet conditions and assumptions of the primary and secondary heat exchangers are generated to perform the calculation of the overall model.

At the end, heat exchanger and compressor models are coupled for cycle modeling. The evolution of the thermodynamic system in steady state conditions is based on a convergence criterion of constant superheat and total amount of refrigerant charge. The superheat at the evaporator outlet is controlled by the expansion device. Therefore, for a given refrigerant mass flow rate, the superheat value sets the evaporating pressure. The refrigerant charge inside the system defines the high pressure level. The total refrigerant charge is split into charges calculated at each iteration, in the evaporator, the condenser, and the refrigerant lines. For the calculation of the refrigerant charge in two-phase flow inside the evaporator and the condenser, an appropriate void fraction model has to be selected. The liquid and vapor masses in an heat-exchanger element of length dL and cross sectional area A are related to the void fraction ε by the following Equations 5 and 6:

$$dC_{VAP} = \rho_V A \times dL \times \varepsilon \quad (5)$$

$$dC_{LIQ} = \rho_L A \times dL \times (1-\varepsilon) \quad (6)$$

In the literature, different void fraction models and correlations have been proposed for the estimation of the void fraction. Newell (Newell *et al.* 2002) have suggested that homogeneous model is most suitable for intermittent flow regimes where bubbles of vapor travel at the same velocity as the liquid slugs. The void fraction is therefore estimated in the micro-channels exchangers using the homogeneous model given by Equation 7.

$$\varepsilon = \left[1 + \left(\frac{1-x}{x}\right)\left(\frac{\rho_V}{\rho_L}\right)\right]^{-1} \quad (7)$$

4. MODELING RESULTS AND DISCUSSION

In this section, the micro-channels heat exchangers (MCHE) model and overall indirect model results are presented in terms of efficiency and components design.

4.1 Comparison to experimental data with plate heat exchangers (PHE)

The relative gains in compactness, related to the use of MCHE, are highlighted by comparison to the experimental data of Shiba et al. (Shiba *et al.* 2007). They presented a development study of a high performance water-to-water heat pump. In their data, they attained a cooling COP of 5.5 by improving the heat exchangers technology, the compressor efficiency, and by integrating a liquid-vapor heat exchanger. Plate heat exchangers with external dimensions 529x268x232 mm^3 (core volume 33 L) were used for the experimental validation.

Table 4: Performance calculation of the developed heat pump (Shiba *et al.* 2007).

Operating Mode	Cold water inlet temp. (°C)	Cold water inlet temp. (°C)	Hot water inlet temp. (°C)	Hot water outlet temp. (°C)	Cooling capacity (kW)	Heating capacity (kW)
Cooling	12	7	25	30	45.6	53.9

The testing conditions of Shiba et al. are used to simulate micro-channels heat exchangers. At equivalent performance, the volumetric flux is presented in Figure 3. The volume of MCHE does not include inlet/outlet distributors. For PHE, the same heat transfer area was used for the evaporator and condenser, which results in a lower volumetric capacity for the evaporator. For MCHE, the same tendency is observed. The volumetric flux is increased by 144 and 154 % in the evaporator and condenser respectively, with the micro-channel technology. No data was reported concerning the pressure drop of water and refrigerant.

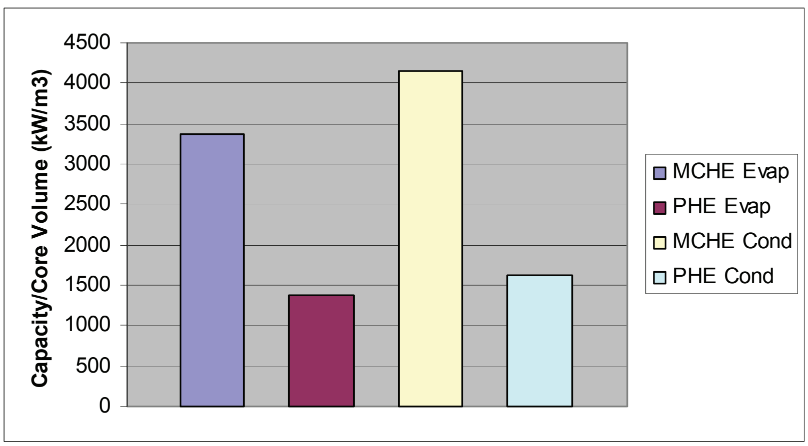

Figure 3: Comparison of the volumetric capacity of MCHE and PHE (Shiba *et al.* 2007).

4.2 Indirect system model results and comparison

The performance of the indirect system was compared to a base case data performance of a direct expansion direct system. The direct system performance is presented in Table 5. The direct system operates with R-407C. The compressor displacement rate is 28.8 m^3/h. The heat-exchanger technology is a conventional finned-tube coil. The external air flow rates are fixed by the machine at 4000 m^3/h at the cooler and 8000 m^3/h at the radiators. The air inlet temperatures are given in Table 5.

Table 5: Comparison of direct to indirect system performances.

System	Air inlet conditions (°C)**	Cold water regime (°C)	Hot water regime (°C)	Cooling capacity (kW)	Sensible /Latent cooling (%)	Heating capacity (kW)	Cooling COP	Refrigerant charge (g/kW)
Direct	42/33/51.5	-	-	31.2	55/45	41.4	3.1	400
Indirect	42/33/51.5	20/16.1	53.3/60.2	31.2	65/35	40.8	3.2	10

**Outdoor air temperature (°C)/ Indoor air temperature (°C)/ indoor air relative humidity (%)

The optimized indirect system performance is presented in Table 5. The results show that same cooling capacity and COP are achieved with the indirect system. The compressor displacement rate is 35.2 m^3/h. Figure 4 presents the temperature levels achieved with the direct and the indirect systems, as well as the optimized HTF inlet/outlet temperatures for TG matching. The average evaporating temperature of the indirect system is 13.4 °C, while that of the direct system is 11 °C. This result suggests that the evaporator is undersized. The average condensing temperature of the direct system is 58.2 °C compared to 61.6°C in the indirect system. The thermodynamic cycle is shifted upwards with the increase of evaporating temperature in the indirect system. The compression ratio is increased from 3.6 to 3.7.

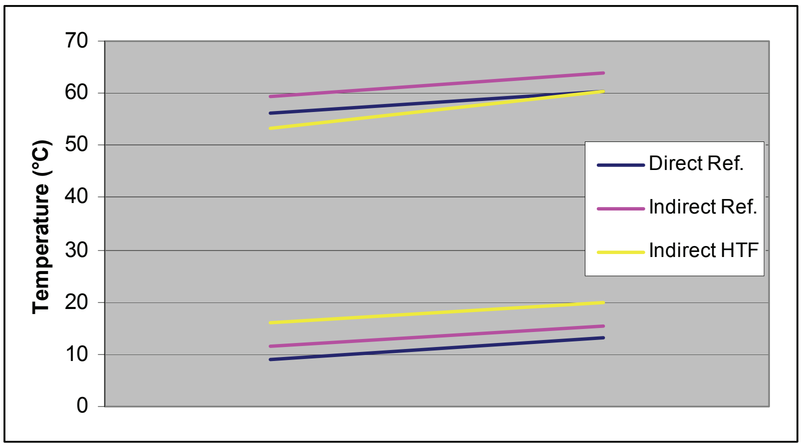

Figure 4: Comparison of direct and indirect cycle temperatures.

The results presented below are related to the primary micro-channels heat exchangers. The simulated heat exchanger geometrical configurations are presented in Table 6.

Table 6: Micro-channels HTF/REF HX characteristics data.

	Evaporator model	Condenser model
Flow arrangement	Counter-flow	Counter-flow
HX length mm	0.4	0.4
HX width mm	0.2	0.22
Number of plates	102	102
Channel D_h (HTF/REF) mm	1/0.5	1/0.5
Channels number / Plate (HTF/REF)	146/220	133/200
Effective area(HTF/REF) m²	10.8/8	11.9/8.8

The evaporator and the condenser volumes are respectively 10.1 and 11.1 L. The volumetric fluxes are 3000 and 3500 kW/m^3. The compactness of the exchangers is around 1900 m^2/m^3. The flow regime is laminar. Table 6 shows that the refrigerant charge is 10 g/kW. The charge calculation excludes the volume of headers. In two-phase flow, the charge is estimated by the homogeneous model.

5. CONCLUSIONS AND PERSPECTIVES

The performance of an indirect air conditioning system operating with a zeotrope mixture R-152a/R-32 (80/20%) has been evaluated through an accurate modeling of primary and secondary heat exchangers. The micro-channel technology has been introduced to primary heat exchangers. The simulations show that an indirect system can be as efficient as a direct system by reducing the minimum approach in heat exchangers.
The modeling correlations for zeotropic mixtures in micro-channels are insufficient and need further research work. Well-known correlations developed for evaporation and condensation of pure refrigerants have been used. Knowing that heat transfer coefficient of zeotropic mixtures is reduced compared to pure components, experimental validation is necessary. This work will be the subject of a future investigation.

NOMENCLATURE

Nomenclature			**Subscripts**		
A	cross sectional area	m^2	w	wall	
D	diameter	m	sat	saturation	
D	displacement rate	m^3/h	l	liquid	
dC	element charge	kg	v	vapor	
G	mass flux	kg/m^2s	cpr	compressor	
g	gravitational acceleration	m/s^2			
h	enthalpy	kJ/kg	**Greek letters**		
h	heat transfer coefficient	$W/K.m^2$	ρ	density	kg/m^3
hfg	vapor liquid enthalpy	kJ/kg	η_v	volumetric efficiency	
k	thermal conductivity	W/K.m	η_{is}	isentropic efficiency	
P	pressure	Pa	υ	specific volume	m^3/kg
q	heat flux	W/m^2	ε	void fraction	
x	vapor quality		ε	efficiency	
			μ	dynamic viscosity	Pa.s

REFERENCES

S. S. Bertsch, E. Groll, S. Garimella, 2008, Refrigerant flow boiling heat transfer in parallel microchannels as a function of local vapor quality, Heat Mass Transfer.
A. Cavallini, D. Del Col, L. Doretti, M. Matkovic, L. Rossetto, C. Zilio, 2005, Condensation heat transfer and pressure gradient inside Multiport Minichannels, Heat Transf. Eng., vol. 26, no. 3, p. 45-55.
A. Cavallini, L. Doretti, M. Matkovic, L. Rossetto, 2006, Update on condensation heat transfer and pressure drop inside Minichannels, Heat Transf. Eng., vol. 27, no. 4, p. 74-87.
V. Dupont, J.R. Thome, A.M. Jacobi, 2004, Heat transfer model for evaporation in microchannels. Part 2: comparison with the database, Heat Mass Transfer, vol. 47, p. 3387-3401.
S. Koyoma, K. Kuwahara, K. Nakashita, K. Yamamoto, 2003, An experimental study on condensation of refrigerant R-134a in a multi-port extruded tube, Int. J. Refrig., vol 24, p.425-432.
W. J. Mulroy, P.A. Domanski, D. A. Didion, 1994, Glide matching with binary and ternary zeotropic refrigerant mixtures, Part 1. An experimental study, Int. J. Refrig., vol. 17, no. 4, p. 220-225.
Y. Shiba, R. Ooka, Development of a high performance water-to-water heat pump for ground source application, 2007, Ashrae transactions, vol. 113, part 2.
J.R. Thome, 1996, Boiling of new refrigerants: a state of the art review, Int. J. Refrig., vol. 19, no. 7, p. 435-457.
J.R. Thome, V. Dupont, A.M. Jacobi, 2004, Heat transfer model for evaporation in microchannels. Part 1: presentation of the model, Heat Mass Transfer, vol. 47, p. 3375-3385.
G. Venkatarathnam, G. Mokashi, S. Murthy, 1996, Occurrence of pinch points in condensers and evaporators for zeotropic refrigerant mixtures, Int. J. Refrig., vol. 19, no. 6, p. 361-368.
W. W. Wang, T. D. Radcliff, R. Christensen, 2002, A condensation heat transfer correlation for millimeter-scale tubing with flow regime transition, Exp. Thermal Fluid Science, vol. 26, p.473-485.